International Journal of Advanced Engineering Research and Science (IJAERS)
Peer-Reviewed Journal
ISSN: 2349-6495(P) | 2456-1908(O)
Vol-13, Issue-2; Feb, 2026
Journal Home Page Available: https://ijaers.com/
Article DOI: https://dx.doi.org/10.22161/ijaers.132.2

Energy Loss Coefficient Equation in the Modified Euler Momentum Conservation Equation for A Time-Series Water Wave Model

Syawaluddin Hutahaean

Ocean Engineering Program, Faculty of Civil and Environmental Engineering-Bandung Institute of Technology (ITB), Bandung 40132, Indonesia.

syawalf1@yahoo.co.id

Received: 30 Dec 2025,

Received in revised form: 01 Feb 2026,

Accepted: 06 Feb 2026,

Available online: 11 Feb 2026

***Keywords*— energy losses, breaking.**

Abstract— *The modified Euler momentum conservation equation proposed by the author contains a term that represents wave energy dissipation. This term includes an energy loss coefficient that governs the magnitude of energy release. The coefficient is not a constant but a function of hydrodynamic parameters; therefore, an explicit formulation of this coefficient is required. In this study, the energy loss coefficient is derived using the Kinematic Free Surface Boundary Condition, incorporating wave energy, wavelength, and wave period as governing parameters. The resulting formulation enables effective representation of energy dissipation within the modified Euler momentum conservation equation. Consequently, a time-series water wave model is obtained that is capable of realistically passing through the breaking phase and propagating into shallower waters.*

I. INTRODUCTION

As ocean waves propagate toward coastal waters, they undergo progressive energy dissipation. Well-established mechanisms of wave energy loss include bottom friction, viscosity, radiation stress, and wave breaking. While formulations describing energy dissipation due to bottom friction, viscosity, and radiation stress are widely available, a definitive expression for energy release during wave breaking remains limited, despite the fact that breaking accounts for a substantial portion of total wave energy dissipation. Consequently, for a time-series wave model to realistically pass through the breaking phase and continue propagating into shallower waters, an appropriate formulation of breaking-induced energy dissipation is required.

Hutahaean (2025a) proposed a modified Euler momentum conservation equation incorporating a total energy dissipation term. In that study, however, the energy loss coefficient was determined through a trial-and-error approach. The present study advances this formulation by deriving the energy dissipation coefficient in a more systematic manner based on the Kinematic Free Surface Boundary Condition.

Using velocity potential theory, Hutahaean (2023, 2025b) derived a relationship referred to as the wave amplitude function, which successfully captures key characteristics of wave breaking and the shoaling–breaking process. This relationship provides the theoretical foundation for developing the energy dissipation coefficient proposed in this study.

The effectiveness of wave energy dissipation formulations can be evaluated through their ability to predict breaking wave height. Accordingly, breaking wave height is adopted in this study as the primary benchmark for assessing the accuracy of the developed energy loss coefficient.

Numerous previous studies have proposed empirical formulations for breaking wave height using deep-water wave height, deep-water wavelength, and bottom slope as input parameters. Notable contributions include those by Le Méhauté and Koh (1967), Komar and Gaughan (1972), Sunamura and Horikawa (1974), Singamsetti and Wind (1980), Ogawa and Sutto (1984), Larson and Kraus (1989), Smith and Kraus (1990), Gourlay (1992), and Rattana Pitikon and Shibayama (2000).

II. MODIFIED EULER MOMENTUM CONSERVATION EQUATION.

Hutahaean (2025a) formulated a modified Euler momentum equation derived using a control volume approach and evaluated at a control point, as illustrated in Fig (2).

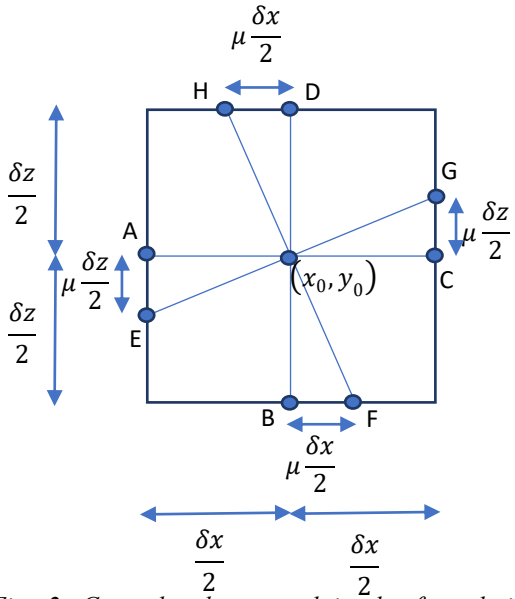

Fig. 2. Control volume used in the formulation of the modified Euler momentum conservation equation.

The acceleration in the horizontal-x direction is defined as the difference between the velocities at points E and G, while the corresponding driving force is given by the pressure difference between points C and A. Similarly, the acceleration in the vertical-z direction is defined as the difference between the vertical velocities at points F and H, with the driving force represented by the pressure difference between points B and D. Accordingly, the momentum conservation equations in the horizontal-x and vertical-z directions are obtained by sequentially applying the irrotational flow assumption.

$$\frac{\partial u}{\partial t} + \frac{1}{2}\frac{\partial}{\partial x}(uu + \mu ww) = -\frac{1}{\rho}\frac{\partial p}{\partial x}$$
$$\frac{\partial w}{\partial t} + \frac{1}{2}\frac{\partial}{\partial z}(-\mu uu + ww) = -\frac{1}{\rho}\frac{\partial p}{\partial z} - g$$

By applying a weighted Taylor series expansion, the momentum conservation equations can be written as

$$\gamma_{t,3}\frac{\partial u}{\partial t} + \frac{\gamma_{x,3}}{2}\frac{\partial}{\partial x}(uu + \mu ww) = -\frac{1}{\rho}\frac{\partial p}{\partial x}$$
$$\gamma_{t,3}\frac{\partial w}{\partial t} + \frac{\gamma_{z,3}}{2}\frac{\partial}{\partial z}(-\mu uu + ww) = -\frac{1}{\rho}\frac{\partial p}{\partial z} - g$$

$\gamma_{t,3}$, $\gamma_{x,3}$ and $\gamma_{z,3}$ are the weighting coefficients of the weighted Taylor series for a function $f = f(x, z, t)$, with $\gamma_{t,3} = 3.04933., \gamma_{x,3} = \gamma_{z,3} = 2.04933$, Hutahean (2025b).

The second terms on the left-hand side represent the convective acceleration. These terms are interpreted as hydrodynamic forces acting in the direction from higher to lower energy. Accordingly, Hutahaean (2025c) argued that these terms should carry a negative sign (-), yielding

$$\gamma_{t,3}\frac{\partial u}{\partial t} - \frac{\gamma_{x,3}}{2}\frac{\partial}{\partial x}(uu + \mu ww) = -\frac{1}{\rho}\frac{\partial p}{\partial x} \quad \ldots.(1)$$
$$\gamma_{t,3}\frac{\partial w}{\partial t} - \frac{\gamma_{z,3}}{2}\frac{\partial}{\partial z}(-\mu uu + ww) = -\frac{1}{\rho}\frac{\partial p}{\partial z} - g \ldots.(2)$$

Equations (1) and (2) constitute the modified Euler momentum conservation equations. The energy dissipation terms are identified as $\frac{\partial \mu uu}{\partial z}$ dan $\frac{\partial \mu ww}{\partial x}$.

Hutahaean (2025a) demonstrated that μ represents an energy loss coefficient. The study further showed that a distortion of the coordinate system relative to the original axes, quantified by μ arises from energy instability or imbalance. To restore equilibrium, energy dissipation occurs, with the magnitude of the distortion depending on the amount of energy released. Consequently, μ is an energy-dependent loss coefficient and is not a constant; rather, it is a function of space and time, expressed as $\mu = \mu(x, t)$.

III. ENERGY LOSS COEFFICIENT EQUATION $\mu(x, t)$.

3.1. Velocity Potential Theory.

Using velocity potential theory, Hutahaean (2023, 2025b) derived a relationship referred to as the wave amplitude function by integrating the Kinematic Free Surface Boundary Condition with respect to time. The resulting expression is,

$$A = \frac{2\,Gk}{\gamma_{t,2}\sigma}\cosh\theta\pi\left(1 - \gamma_{x,2}\frac{kA}{2}\right) \quad \ldots(3)$$

where A is the wave amplitude, G is the wave energy transmission rate representing the kinetic energy of the wave, and k is the wave number defined as $k = \frac{2\pi}{L}$, with L

denoting the wavelength. The angular frequency $\sigma = \frac{2\pi}{T}$, where T is the wave period. The coefficients $\gamma_{t,2} = 1.9973$ and $\gamma_{x,2} = 0.9973$ are weighting coefficients of the weighted Taylor series for a function $f = f(x,t)$, (Hutahaean, 2025b).

Shoaling–breaking processes modeled using Eq. (3) exhibit automatic wave breaking when the following condition is satisfied:
$1 - \gamma_{x,2}\frac{kA}{2} = 0.$

After breaking, the wave height decreases continuously until it vanishes. This post-breaking decay of wave height (or wave amplitude) is governed by the same term $\left(1 - \gamma_{x,2}\frac{kA}{2}\right)$, where increasing water shallowness corresponds to larger values of the wave number k. The formulation therefore enables direct analysis of wave energy dissipation (Hutahaean, 2025b).

These results indicate that wave energy dissipation is inherently embedded in the Kinematic Free Surface Boundary Condition.

Equation (3) may be rewritten as

$$A = \left(\frac{2\cosh\theta\pi}{\gamma_{t,2}\sigma}\right) Gk\left(1 - \gamma_{x,2}\frac{kA}{2}\right)$$

The term $\left(\frac{2\cosh\theta\pi}{\gamma_{t,2}\sigma}\right)$ represents deep-water wave characteristics, G characterizes wave energy, k reflects wavelength variation in shallow water, and $\left(1 - \gamma_{x,2}\frac{kA}{2}\right)$ represents the Kinematic Free Surface Boundary Condition.

3.2. Formulation of the Energy Loss Coefficient

As discussed in the previous section, the energy loss coefficient depends on deep-water wave conditions, wave energy, and the Kinematic Free Surface Boundary Condition. The weighted form of the Kinematic Free Surface Boundary Condition is expressed as,

$$\gamma_{t,2}\frac{\partial\eta}{\partial t} = w_\eta - \gamma_{x,2}u_\eta\frac{\partial\eta}{\partial x} \quad \ldots(4)$$

Accordingly, the general form of the energy loss coefficient $\mu(x,t)$ is,

$$\mu(x,t) = c(H_0, L_0)\left(\frac{u_\eta u_\eta + w_\eta w_\eta}{2g}\right)\left(\frac{w_\eta - \gamma_{x,2}u_\eta\frac{\partial\eta}{\partial x}}{\gamma_{t,2}}\right)k$$

$c(H_0, L_0)$ represents deep-water wave conditions, $\left(\frac{u_\eta u_\eta + w_\eta w_\eta}{2g}\right)$ denotes the kinetic energy of the wave $\left(\frac{w_\eta - \gamma_{x,2}u_\eta\frac{\partial\eta}{\partial x}}{2g}\right)$ corresponds to the Kinematic Free Surface Boundary Condition, and, k is wave number.

Using the wave-number conservation relation proposed by Hutahaean (2023), the following relationship holds:

$$k\left(h + \frac{A}{2}\right) = \theta\pi$$

In shallow water, wave amplitude A is unidentified; therefore, the wave number is approximated as:

$$k = \frac{\theta\pi}{h + \eta} \quad \ldots(5)$$

The term $c(H_0, L_0)$ which characterizes deep-water wave conditions, is expressed as $c_\mu\left(\frac{H_0}{L_0}\right)\sigma^3$ where c_μ is an empirically determined coefficient obtained through trial-and-error calibration. The factor σ^3 represents wave-period dependence, with the exponent also determined empirically. The wave period is not arbitrarily specified but is computed using deep-water wave height as input.

$$\alpha = \frac{2\left(2 - \sqrt{2}\right)\tanh\theta\pi}{\gamma_{x,2}H_0}$$

$$\sigma^2 = 1.119\left(-\gamma_{x,2}\alpha\frac{H_0}{2} + \tanh\theta\pi\right)\frac{g\alpha}{\gamma_{t,2}\gamma_{t,3}} \quad \ldots(6)$$

Deep water wavelength is calculated using the following formula,

$$\frac{H_0}{L_0} = 0.131929 \quad \ldots.(7)$$

Deep water depth,

$$h_0 = \frac{\theta\pi}{k_0} - \frac{H_0}{4} \quad \ldots(8)$$

Equations (6). (7) and (8) are derived using velocity potential theory. The parameter θ is the deep-water coefficient, for which $\tanh\theta\pi \approx 1.0$ in deep-water conditions. In shallow water, the wave number k is evaluated as

$$k = \frac{\theta\pi}{h + \eta}$$

Hence, the final expression for the energy dissipation coefficient is,

$$\mu(x,t) = c_\mu\sigma^3\left(\frac{H_0}{L_0}\right)\left(\frac{u_\eta u_\eta + w_\eta w_\eta}{2g}\right)\left(\frac{w_\eta - \gamma_{x,2}u_\eta\frac{\partial\eta}{\partial x}}{\gamma_{t,2}}\right)\frac{\theta\pi}{h + \eta} \quad \ldots(9)$$

The coefficient $c_\mu = 0.96\ sec^4m^{-1}$ and σ^3 dependence, is obtained by calibrating the predicted breaking wave height against the mean breaking wave height derived from

empirical formulations reported in previous studies (see Section 5.4). In Eq. (9), bottom slope does not explicitly appear, as its influence is implicitly incorporated through the water-particle velocities and the free-surface elevation η and $\frac{\partial \eta}{\partial x}$.

IV. TIME-SERIES WAVE MODEL EMPLOYED

The time-series wave hydrodynamic model consists of two governing equations: the water surface elevation equation and the depth-averaged horizontal water-particle velocity equation.

The water surface elevation equation is formulated as a superposition of the continuity equation and the kinetic energy conservation equation. The derivation and detailed formulation are presented in Hutahaean (2025a, 2025d). In the present study, the kinetic energy conservation equation is modified to account for energy dissipation, yielding

$$\frac{\partial E_k}{\partial t} = -\frac{\gamma_{x,3}}{1+\mu}\frac{\partial u E_{kx}}{\partial x} - \frac{\mu\gamma_{x,3}}{1+\mu}\frac{\partial u E_{kx}}{\partial z} - \frac{\gamma_{z,3}}{1+\mu}\frac{\partial w E_{kz}}{\partial z} + \frac{\mu\gamma_{z,3}}{1+\mu}\frac{\partial w E_{kz}}{\partial x}$$

$E_k = E_{kx} + E_{kz}$, is the horizontal kinetic energy $E_{kx} = \frac{u^2}{2g}$, is the horizontal kinetic energy $E_{kz} = \frac{w^2}{2g}$.

The depth-averaged horizontal water-particle velocity equation is formulated as a superposition of the modified Euler momentum conservation equation and the momentum equilibrium equation. The derivation and complete formulation of this equation are provided in Hutahaean (2025a).

V. MODEL RESULTS

5.1. Coefficients in the Model.

Two coefficients (or constants) are employed in the model: the deep-water coefficient θ and the depth-averaging coefficient ε_z.

a. Deep water coefficient θ

The appropriate value of θ is determined such that, for simulations over a flat bottom without energy dissipation, the wave height remains unchanged during propagation. If θ is chosen too small, wave height amplification occurs; conversely, excessively large values of θ lead to wave height attenuation.

b. Depth-Averaging Integrating Coefficient.

The model employs a depth-averaged velocity defined as the water-particle velocity evaluated at an elevation z_0 below the still water level (Hutahaean, 2025d). In this study, $z_0 = -0.45\, h_0$ is adopted. Defining $\varepsilon_z = \left|\frac{z_0}{h_0}\right|$, a value of $\varepsilon_z = 0.45$ is used to compute the integration and transformation coefficients. The governing expressions for these coefficients are provided in Hutahaean (2025d).

5.2. Input Wave Profile.

The input wave is prescribed using a solitary wave profile, which satisfies the initial conditions at the input boundary, $\eta(0,0) = \frac{\partial \eta}{\partial t} = 0$. The input wave elevation is defined as

$\eta(0,t) = -\frac{H_0}{2}\cos\sigma t + \frac{H_0}{2}$

Fig (2) illustrates the input wave profile as a function of time for $H_0 = 2.40\ m, T = 8.0\ sec$.

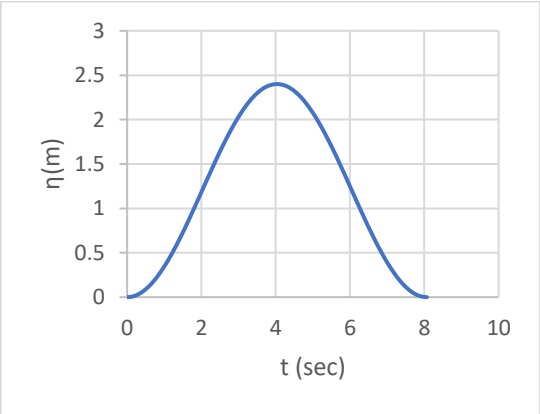

Fig (2). Input wave profile as a function of time t

5.3. Example of Shoaling–Breaking Model Output

This section presents selected model outputs illustrating the shoaling–breaking process over a bottom slope of $m = 0.04$, together with wave profiles at the breaking point and in shallow water. Simulations are conducted for waves with $H_0 = 1.20\ m$, $T = 5.656\ sec.$, $H_0 = 2.40\ m$, $T = 8.00\ sec.$ and $H_0 = 3.60\ m, T = 9.797\ sec.$ In the figures, the crest line denotes the curve connecting successive wave crests. The upper ordinate limit in each plot corresponds to the breaking wave height; consequently, the crest line is tangent to the upper ordinate boundary.

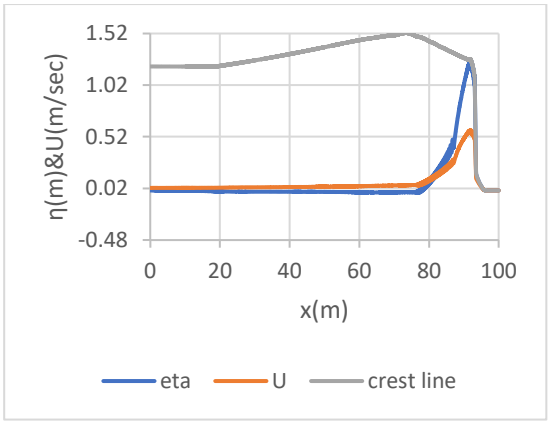

Fig. (3) Shoaling breaking, $H_0 = 1.20\ m$, $T = 5.656\ sec.$, $m = 0.04$

A steady positive current is observed in the wave trough region, indicating flow in the direction of wave propagation. This current is presumed to result from radiation stress.

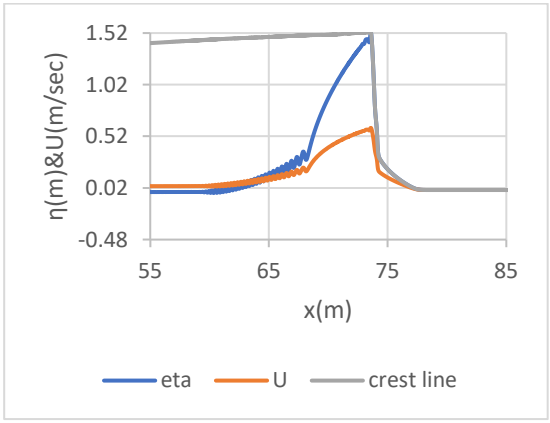

Fig. (4) Wave profile at breaking point $h_b = 2.08\ m$,$H_0 = 1.20\ m$, $m = 0.04$

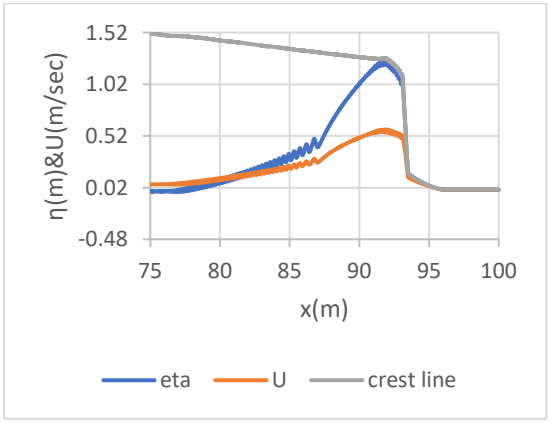

Fig. (5) Wave profile at shallow water $h = 1.32\ m$,$H_0 = 1.20\ m$, $m = 0.04$

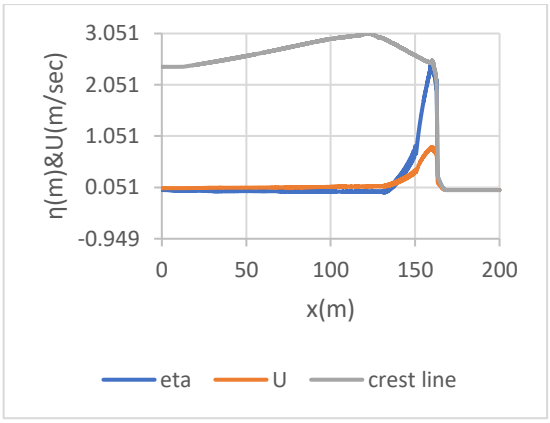

Fig. (6) Shoaling breaking, $H_0 = 2.40\ m$, $T = 8.0\ sec.$, $m = 0.04$

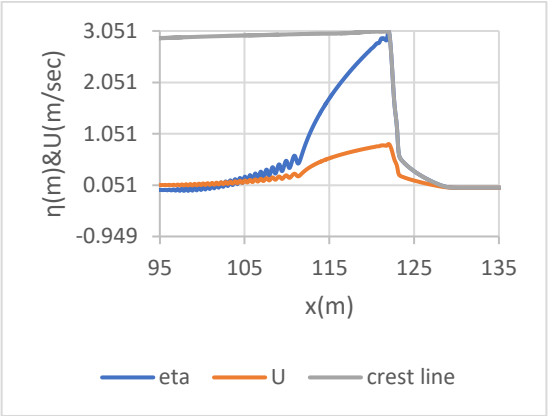

Fig. (7) Wave profile at breaking point $h_b = 4.128\ m$,$H_0 = 2.40\ m$, $m = 0.04$

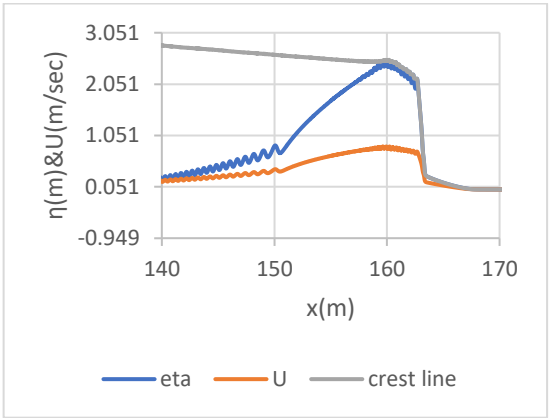

Fig. (8) Wave profile at shallow water $h = 2.60\ m$,$H_0 = 2.40\ m$, $m = 0.04$

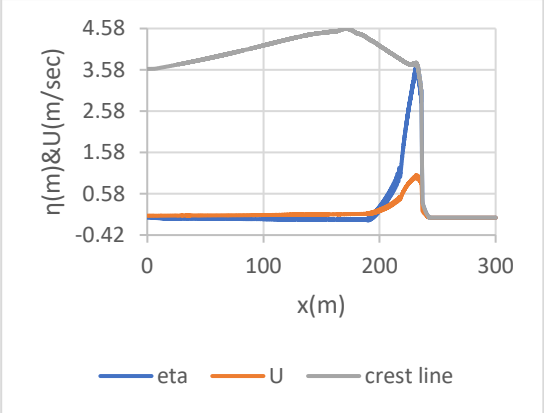

Fig. (9) Shoaling breaking, $H_0 = 3.60\ m$, $T = 9.797\ sec.$, $m = 0.04$

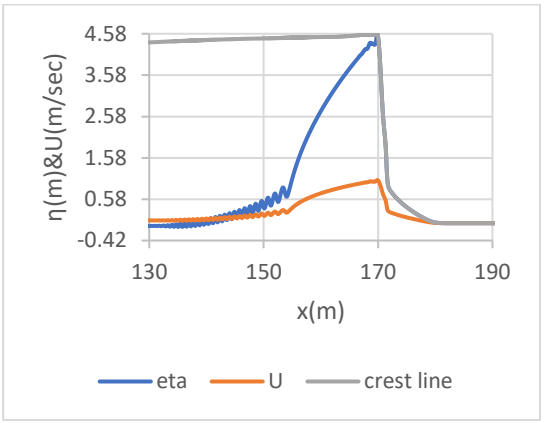

Fig. (10) Wave profile at breaking point $h_b = 6.164\ m$,$H_0 = 3.60\ m$, $m = 0.04$

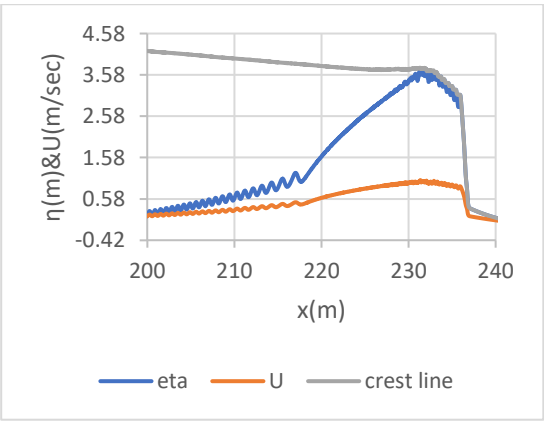

Fig. (11) Wave profile at shallow water $h = 3.60\ m$,$H_0 = 3.60\ m$, $m = 0.04$

5.4. Evaluation of Breaking Conditions in the Model.

The model performance and the proposed energy dissipation formulation are evaluated by examining the predicted breaking wave height. Model-derived breaking wave heights are compared with those obtained from empirical formulations proposed by previous researchers.

5.4.1. Breaking wave height equations from previous researchers.

Several studies have established relationships between breaking wave height H_b and deep-water wave height H_0.

a. Le Mehaute and Koh (1967).

$$\frac{H_b}{H_0} = 0.76 \left(\frac{H_0}{L_0}\right)^{-1/4} m^{1/7}$$

b. Komar and Gaughan (1972).

$$\frac{H_b}{H_0} = 0.56 \left(\frac{H_0}{L_0}\right)^{-1/5}$$

c. Sunamura and Horikawa (1974).

$$\frac{H_b}{H_0} = \left(\frac{H_0}{L_0}\right)^{-1/4} m^{0.2}$$

d. Singamsetti and Wind (1980).

$$\frac{H_b}{H_0} = 0.575 \left(\frac{H_0}{L_0}\right)^{-0.254} m^{0.031}$$

e. Ogawa and Sutto (1984).

$$\frac{H_b}{H_0} = 0.68 \left(\frac{H_0}{L_0}\right)^{-1/4} m^{0.09}$$

f. Larson and Kraus (1989).

$$\frac{H_b}{H_0} = 0.53 \left(\frac{H_0}{L_0}\right)^{-0.24}$$

g. Smith and Kraus (1990).

$$\frac{H_b}{H_0} = (0.34 + 2.47\ m) \left(\frac{H_0}{L_0}\right)^{-0.3+0.88\ m}$$

h. Gourlay (1992).

$$\frac{H_b}{H_0} = 0.478 \left(\frac{H_0}{L_0}\right)^{-0.28}$$

i. Rattana Pitikon and Shibayama (2000).

$$\frac{H_b}{H_0} = (10.02\ m^3 - 7.46\ m^2 + 1.32\ m + 0.55) \left(\frac{H_0}{L_0}\right)^{-1/5}$$

m is bottom slope, L_0 is deep water wave length from the linear wave theory as follows,

$k_0 = \frac{\sigma^2}{g}$, $L_0 = \frac{2\pi}{k_0}$.

As a reference for model validation, the mean value of the breaking wave height H_b derived from the nine empirical formulations is adopted. The average breaking wave heights for bottom slopes $m = 0.04$, $m = 0.05$ and $m = 0.06$ are presented in Table 1. The results indicate that steeper bottom slopes produce slightly higher breaking wave heights, although the increase is limited to only a few centimeters.

Table (1). Average Breaking Wave Height

H_0 (m)	T (sec)	$H_{b,0.04}$ (m)	$H_{b,0.05}$ (m)	$H_{b,0.06}$ (m)
1.2	5.656	1.526	1.55	1.57

1.6	6.532	2.035	2.067	2.093
2	7.302	2.544	2.583	2.617
2.4	7.999	3.053	3.1	3.14
2.8	8.64	3.562	3.617	3.663
3.2	9.237	4.07	4.133	4.187
3.6	9.797	4.579	4.65	4.71

Note: $H_{b,x.xx}$, $x.xx$ = bottom slope

5.4.2. Comparison of Breaking Wave Height.

Tables 2, 3, and 4 present comparisons between the model-predicted breaking wave height and the mean breaking wave height derived from previous empirical studies for bottom slopes $m = 0.04$, $m = 0.05$ dan $m = 0.06$ respectively.

For a bottom slope of $m = 0.04$, the model results are slightly lower than those reported in previous studies, with differences ranging from 0.000 to 0.007 m. At $m = 0.05$, the model predictions are not consistently lower; in some cases, they exceed the empirical values, with differences in the range of 0.000–0.005 m. In contrast, for $m = 0.06$, the model consistently yields higher breaking wave heights than the empirical formulations, with differences ranging from 0.005 to 0.012 m. These discrepancies are very small and can be considered negligible.

The close agreement between the model predictions and the empirical formulations is attributed to the consistent determination of wave period in both approaches. In this study, the wave period is computed from the wave amplitude using Eq. (6), rather than being arbitrarily prescribed. Based on these results, it can be concluded that the energy dissipation formulation proposed in this study provides accurate and reliable predictions of breaking wave height.

Table (2). Comparison of breaker height for bottom slope $m = 0.04$

H_0 (m)	T (sec)	$H_{b,0.04}$ (m)	$H_{b,m}$ (m)	$H_{b,m} - H_{b,0.04}$ (m)
1.2	5.656	1.526	1.525	-0.001
1.6	6.532	2.035	2.03	-0.005
2	7.302	2.544	2.544	0
2.4	7.999	3.053	3.051	-0.002
2.8	8.64	3.562	3.555	-0.007
3.2	9.237	4.07	4.07	0
3.6	9.797	4.579	4.576	-0.003

Note: H_{b-m}: H_b model

Table (3). Comparison of breaker height for bottom slope $m = 0.05$

H_0 (m)	T (sec)	$H_{b,0.05}$ (m)	$H_{b,m}$ (m)	$H_{b,m} - H_{b,0.05}$ (m)
1.2	5.656	1.55	1.553	0.003
1.6	6.532	2.067	2.066	-0.001
2	7.302	2.583	2.588	0.005
2.4	7.999	3.1	3.1	0
2.8	8.64	3.617	3.616	-0.001
3.2	9.237	4.133	4.133	0
3.6	9.797	4.65	4.648	-0.002

Note: H_{bm}: H_b model

Table (4). Comparison of breaker height for bottom slope $m = 0.06$

H_0 (m)	T (sec)	$H_{b,0.06}$ (m)	$H_{b,m}$ (m)	$H_{b,m} - H_{b,0.06}$ (m)
1.2	5.656	1.57	1.58	0.01
1.6	6.532	2.093	2.101	0.008
2	7.302	2.617	2.629	0.012
2.4	7.999	3.14	3.149	0.009
2.8	8.64	3.663	3.668	0.005
3.2	9.237	4.187	4.197	0.01
3.6	9.797	4.71	4.717	0.007

Note: H_{bm}: H_b model

5.4.3. Studies on Breaker Depth Index.

The breaker depth index defined as $\frac{H_b}{h_b}$, H_b is the breaking wave height and h_b is the water depth at the breaking point, has received considerable attention in breaking-wave research. This parameter is particularly important for characterizing nearshore wave conditions. The model-derived breaker depth indices are presented in Tables 5, 6, and 7 for bottom slopes $m = 0.04$, $m = 0.05$ and $m = 0.06$ respectively.

For a bottom slope of $m = 0.04$, the mean value of $\frac{H_b}{h_b}$ is 0.74. This value increases to an average of 0.80 for $m = 0.05$ and to 0.86 for $m = 0.06$. These results indicate that the breaker depth index increases with increasing bottom slope. All values are in close agreement with the classical criterion proposed by McCowan (1894), which suggests average $\frac{H_b}{h_b} = 0.78$.

In the present model, $\frac{H_b}{h_b}$ is influenced not only by bottom slope but also by deep-water wavelength. Shorter deep-water wavelengths lead to larger values of the breaker depth index.

Table (5) Breaker depth index $\frac{H_b}{h_b}$, at bottom slope $m =$ 0.04

H_0 (m)	T (sec)	H_b (m)	h_b (m)	$\frac{H_b}{h_b}$
1.2	5.656	1.525	2.080	0.733
1.6	6.532	2.030	2.747	0.739
2	7.302	2.544	3.436	0.741
2.4	7.999	3.051	4.128	0.739
2.8	8.64	3.555	4.797	0.741
3.2	9.237	4.070	5.486	0.742
3.6	9.797	4.576	6.164	0.742

Note: h_b, breaker depth

Table (6) Breaker depth index $\frac{H_b}{h_b}$, at bottom slope $m =$ 0.05

H_0 (m)	T (sec)	H_b (m)	h_b (m)	$\frac{H_b}{h_b}$
1.2	5.656	1.553	1.934	0.803
1.6	6.532	2.066	2.578	0.801
2	7.302	2.588	3.222	0.803
2.4	7.999	3.100	3.859	0.803
2.8	8.64	3.616	4.494	0.805
3.2	9.237	4.133	5.134	0.805
3.6	9.797	4.648	5.781	0.804

Note: h_b, breaker depth

Table (7) Breaker depth index $\frac{H_b}{h_b}$, at bottom slope $m =$ 0.06

H_0 (m)	T (sec)	H_b (m)	h_b (m)	$\frac{H_b}{h_b}$
1.2	5.656	1.580	1.843	0.857
1.6	6.532	2.101	2.436	0.862
2	7.302	2.629	3.091	0.850
2.4	7.999	3.149	3.655	0.862
2.8	8.64	3.668	4.241	0.865
3.2	9.237	4.197	4.885	0.859
3.6	9.797	4.717	5.486	0.860

Note: h_b, breaker depth

VI. CONCLUSIONS

The first conclusion of this study is that the modified Euler momentum conservation equation contains terms that represent wave energy dissipation. The coefficient associated with these terms can be systematically derived using the Kinematic Free Surface Boundary Condition. The resulting energy dissipation coefficient yields breaking wave heights that are consistent with those reported in previous studies.

It can therefore be concluded that the energy dissipation coefficient formulated based on the Kinematic Free Surface Boundary Condition is appropriate for time-series water wave modeling and provides reliable results.

However, the present model is not yet capable of simulating shoaling–breaking processes in very shallow water. Further research is required to improve both the governing equations and the energy dissipation coefficient in order to extend the model's applicability to extremely shallow coastal regions.

REFERENCES

[1] Hutahaean, S. (2025a). Time Series Water Wave Modeling using a Modified Euler Momentum Conservation Equation and a Momentum Equilibrium Equation. International Journal of Advance Engineering Research and Science (IJAERS). Vol. 12, Issue 12; Dec, 2025, pp 13-25. Article DOI: https://dx.doi..org/10.22161/ijaers.1212.2.

[2] Hutahaean, S. (2023). Water Wave Velocity Potential on Slopping Bottom in Water Wave Transformation Modeling. International Journal of Advance Engineering Research and Science (IJAERS). Vol. 10, Issue 10; Oct.; 2023, pp 149-157. Article DOI: https://dx.doi..org/10.22161/ijaers.1010.15.

[3] Hutahaean, S. (2025b). New Weighted Taylor Series for Water Wave Energy Loss and Littoral Current Analysis. International Journal of Advance Engineering Research and Science (IJAERS). Vol. 12, Issue 1; Jan, 2025, pp 27-39. Article DOI: https://dx.doi..org/10.22161/ijaers.121.3.

[4] Le Mehaute, B. and Koh, R.C.Y (1967). On the breaking waves arriving at an angle to shore, J.Hydraulic Research 5,1, pp.67-68.

[5] Komar, P.D. and Gaughan, M.K. (1972). Airy Wave Theory and Breaker Height Prediction. Proc. 13rd, Coastal Eng. Conf., ASCE, pp. 405-418.

[6] Sunamura, T. and Horikawa, K. (1974). Two-dimensional beach transformation due to waves, Proc.14th Coastal Eng. Conf., ASCE, pp.920-938.

[7] Singamsetti, S.R. and Wind, H.G. (1980): Charactersitic of Breaking and Shoaling Periodic Waves Normally Incident on to Plane Beaches of Constant Slope. Report M1371, Delft Hydraulic Lab., Delf, The Netherlands, 142 p.

[8] Ogawa, Y. and Shutto, N. (1984). Run-up of Periodics Waves on Beaches of Non-Uniform Slope. Proc. 19th Coastal Eng. Conf., ASCE, pp. 328-344.

[9] Larson, M. and Kraus, N.C. (1989). SBEACH: Numerical Model for Simulating Storm-induced Beach Change. Report 1, Tech.Report CERC-89-9, Waterways Experiment Station, US Army Corps of Engineers, 267 p.

[10] Smith, J.M. and Kraus (1990). Laboratory Study on Macro-Features of Wave Breaking over Bars and Artificial Reefs. Technical Report. CERC-90-12, WES, U.S. Army Corps of Engineers, 232 p/

[11] Gourlay, M.R. (1992). Wave Set-up Wave run-up and Beach Water Table: Interaction between Surf Zone Hydraulics and Groundwater Hydraulics. Coastal Eng. 17, pp.93-144.

[12] Rattanapitikon, W. and Shibayama (2000). Verivication and modification of breaker height formulas, Coastal Eng.Journal, JSCE, 42(4), pp.389-406.

[13] Hutahaean, S. (2025c). Enhanced Time-Series Water Wave Model through Refinement of Convective Acceleration and Driving Force in the Velocity Equation. International Journal of Advance Engineering Research and Science (IJAERS). Vol. 12, Issue 9; Sep, 2025, pp 11-19. Article DOI: https://dx.doi..org/10.22161/ijaers.129.2.

[14] Hutahaean, S. (2025d). Time-Series Water Wave Model based on Energy Conservation. International Journal of Advance Engineering Research and Science (IJAERS). Vol. 12, Issue 10; Oct.; 2025, pp 17-29. Article DOI: https://dx.doi..org/10.22161/ijaers.1210.2.

[15] Mc Cowan, J. (1894). On the highest waves of a permanent type, Philosophical Magazine, Edinburgh 38, 5th Series, pp. 351-358.